Galactic Dynamics in the Era of Large Surveys
Proceedings IAU Symposium No. 353, 2019
M. Valluri & J. A. Sellwood, eds.

doi:10.1017/S1743921319008664

Transverse bar/bulge kinematics with Gaia and VVV

Jason L. Sanders[1], N. Wyn Evans[1], Leigh Smith[1,2] and Philip Lucas[2]

[1]Institute of Astronomy, University of Cambridge, Madingley Road, Cambridge, CB3 0HA, UK
email: jls@ast.cam.ac.uk

[2]School of Physics, Astronomy and Mathematics, University of Hertfordshire, College Lane, Hatfield AL10 9AB, UK

Abstract. We present new results on the Galactic bar/bulge transverse velocity structure using Gaia and the VISTA Variables in Via Lactea (VVV) survey. Gaia is complemented in high extinction regions by the multi-epoch infrared VVV observations for which derived relative proper motions can be tied to Gaia's absolute frame. We extract kinematic maps (both 2D and 3D) of the Galactic bar/bulge, from which we measure the pattern speed of the bar using a novel technique. We focus on the evidence of an X-shaped bulge from the kinematic maps.

Keywords. Galaxy: structure, bulge, kinematics and dynamics, fundamental parameters

The Milky Way's bar/bulge is a crucial driver in the evolution of the Galaxy and is an important example of a pseudo-bulge which can be studied in close detail (with full 3D velocities, abundances, stellar ages etc.). However, its study is complicated by significant extinction and crowding. This makes the Gaia satellite's use somewhat limited (Gaia Collaboration *et al.* (2016, 2018)). The multi-epoch infra-red VVV survey has been used to extract proper motions for bulge stars (Smith *et al.* (2018)) but these are strictly relative due to a lack of background reference sources. Using bright overlapping stars, Gaia's reference frame can be used to produce absolute VVV proper motions †.

Sanders *et al.* (2019a) presented kinematic maps of ~ 45 million red giant stars in the Milky Way's bar/bulge using this combined Gaia and VVV proper motion dataset. We extended and clarified the correlations seen in other more limited surveys (Rattenbury *et al.* (2007); Kozłowski *et al.* (2006)). Using a 2D extinction map, completeness correction and giant luminosity function, we inverted the number counts and proper motion distributions as a function of apparent magnitude to measure the density and mean and variance of the transverse velocity distributions as a function of distance. Using an assumption of triaxiality, we combined 2D velocity results for equivalent points in the bar to find a full 3D velocity map that well matched results from spectroscopic surveys.

A key parameter to describe the bar is its bulk rotation rate, the pattern speed, (Bland-Hawthorn & Gerhard (2016)). Tremaine & Weinberg (1984) presented a method for measuring the pattern speed of external galaxies from spectroscopy via integration of the continuity equation. Sanders *et al.* (2019b) showed how a similar method could be

† This work has made use of data from the European Space Agency (ESA) mission *Gaia* (https://www.cosmos.esa.int/gaia), and observations made with ESO Telescopes at the La Silla or Paranal Observatories under ESO programme ID 179.B-2002.

employed for the Milky Way using transverse velocity data. At each Galactic longitude ℓ, the pattern speed can be estimated as

$$\Omega_{\rm p}(\ell) = \frac{\int {\rm d}s{\rm d}b\, \rho s v_\ell}{\int {\rm d}s{\rm d}b\, \rho s (R_0 \cos\ell - s\cos b)}, \tag{0.1}$$

where b is Galactic latitude, s distance, ρ number density, v_ℓ the (solar reflex corrected) velocity in the Galactic longitude direction and R_0 the distance to the Galactic centre. Sanders *et al.* (2019b) applied this method to data finding consistent results only for the near-side of the Galactic bar ($\ell > 0$), which yielded an estimate of $\Omega_{\rm p} = (41 \pm 3)\,{\rm km\,s^{-1}kpc^{-1}}$.

The X-shaped bulge

The magnitude distribution of high latitude bulge giants has a double peak structure (McWilliam & Zoccali (2010); Nataf *et al.* (2010), see Fig. 1) which has been interpreted as an X-shaped bulge. However, the evidence for an X-shaped morphology has been contested (Joo *et al.* (2017)) and a different interpretation is the bulge contains red clump populations with intrinsically different brightnesses (potentially due to differing helium abundances). We now turn to assessing the presence of the X-shaped structure using the new data from Gaia and VVV.

The double red clump observed by Gaia

López-Corredoira *et al.* (2019) recently analysed Gaia parallax measurements of red clump stars in seven low extinction Galactic bulge regions. Using the median parallaxes (as a claimed unbiased measure of the true average distance) in a series of apparent magnitude bins between $12 < K_s < 14$, these authors found a clear trend in the absolute magnitude with apparent magnitude, whereby the fainter peak of the double red clump is intrinsically ~ 0.4 mag fainter than the brighter peak, thus supporting the multiple populations model. In Fig. 1 we show bulge giants from the VVV survey with $12 < K_s < 14$ in a $0.6 \times 0.6\,{\rm arcmin}^2$ field centred on $(\ell, b) = (0, -8)$ deg. This high-latitude, minor-axis field shows a double red clump feature. The red dashed line of absolute magnitude against apparent magnitude shows the trend from López-Corredoira *et al.* (2019), but with neither red clump peak centred on the expected ~ -1.6 mag for the red clump. As López-Corredoira *et al.* (2019) note, this is likely due to the known parallax systematics from Gaia. We employ a constant shift of 0.04 mas (Lindegren *et al.* (2018)) combined with the K_s dependent gradient $-0.057\,{\rm mas\,mag^{-1}}$ from López-Corredoira *et al.* (2019). This produces the solid red line and the expected absolute magnitude for the bright peak. However, the difference in the absolute magnitude of the two red clump peaks remains.

We use the modelling described in Sanders *et al.* (2019a) to measure the density profile of bulge giants with $12 < K_s < 14$ in a $0.6 \times 0.6\,{\rm arcmin}^2$ field centred on $(\ell, b) = (0, -8)$ deg. From the best-fit model we sample 50,000 stars and the resulting run of absolute magnitude computed using the median parallax is shown by the blue dashed line in Fig. 1. Note in the model, the two red clump peaks have very similar absolute magnitudes although the fainter peak is slightly intrinsically fainter due to greater contamination from the fainter red giant branch stars. We scatter the true parallaxes of the samples using an error model of $\sigma_\varpi = (0.055\,{\rm mas})\exp(0.385(K_s - 13))$ (fitted to the parallax uncertainties σ_ϖ of the data in this field). The results are shown by the solid blue line which has a gradient in the absolute magnitude between the double peaks, neatly matching the data.

https://doi.org/10.1017/S1743921319008664 Published online by Cambridge University Press

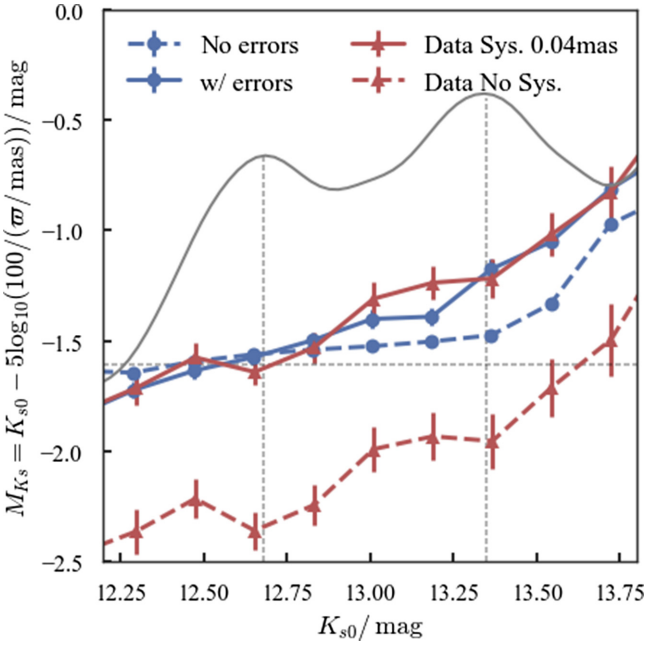

Figure 1. Median absolute magnitude against (extinction-corrected) apparent magnitude computed from the median parallax for bulge giants in a $0.6 \times 0.6\,\mathrm{arcmin}^2$ field centred on $(\ell, b) = (0, -8)$ deg. Solid (dashed) blue is the model with (without) uncertainties and solid (dashed) red is data with (without) a parallax systematic of 0.04 mas applied. The grey line shows a kernel density estimate of the apparent magnitude distribution. Note the data show a difference in the absolute magnitude of the two peaks suggesting two different populations, but this feature is reproduced in the error-convolved single red clump population model.

It is worth briefly understanding why this feature only appears when the mock data are error-convolved. The median parallax is an unbiased measure of the median true parallax only for near-symmetric Gaussian-like distributions. A simple test takes samples from a Gaussian in distance centred at 8 kpc with standard deviation 2 kpc. Convolving the parallax distribution (which is asymmetric with a longer tail to larger parallaxes) with Gaussian uncertainties, we find that the median parallax is biased high which would produce a smaller expected absolute magnitude (for example, uncertainties of 0.2 mas produce an absolute magnitude difference of 0.15 mag). The fainter peak of the double red clump has a significantly asymmetric distribution, primarily due to the increased contamination from background red giant stars, and hence gives rise to a larger systematic.

The kinematics of the double red clump

In response to Gonzalez *et al.* (2015), who argued that the varying weights of the two red clump contributions across the bulge supported the X-shaped scenario, Joo *et al.* (2017) presented a model with a composite bulge composed of two red clump populations with different absolute magnitudes embedded in a bar, which could qualitatively reproduce the data. Both Sanders *et al.* (2019a) and Clarke *et al.* (2019) used proper motions from VVV and Gaia to demonstrate that there are kinematic differences between the two red clump peaks. This supports the X-shaped picture where stars on opposite sides of the bulge stream at different velocities and provides a test of the Joo *et al.* (2017) model.

https://doi.org/10.1017/S1743921319008664 Published online by Cambridge University Press

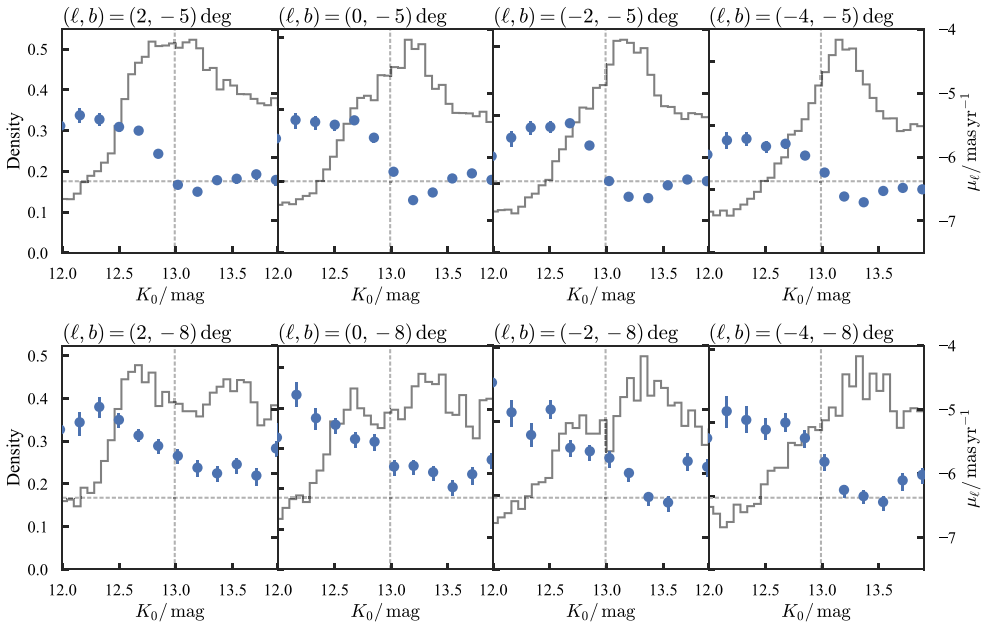

Figure 2. Extinction-corrected magnitude and proper motion distributions for bar/bulge giants in 0.6×0.6 arcmin^2 fields. Grey lines show the number counts and blue dots the median longitudinal proper motion in magnitude bins. The vertical dashed line gives the magnitude of Galactic centre red clump stars and the horizontal dashed line the proper motion of Sgr A*. Note the double peak and differential motion at $b = -8$ deg indicative of the X-shaped bulge.

In Fig. 2 we present the magnitude distributions and median proper motions in the Galactic longitude direction for two sequences of fields at $\ell = (2, 0, -2, -4)$ deg and $b = (-5, -8)$ deg. Both rows show the variation of the red clump contributions as we move from the nearside of the bar (more bright stars at positive longitudes) to the far side. In the higher latitude fields ($b = -8$ deg) the double red clump feature and differential motion between the bright and faint peaks is clear. Interestingly, the fainter peak does not stream faster than Sgr A* indicating potentially that it does not correspond to stars on the far-side of the bar. However, some part of the signal is contamination from fainter red giant branch stars that belong to the nearside of the X. Such an effect is included in the fuller models of Sanders *et al.* (2019a) and Clarke *et al.* (2019).

Sanders *et al.* (2019a) presented a single panel of this figure (second lower) which could be interpreted as supporting the Joo *et al.* (2017) model (see their figure 11). If the bright peak is composed of bar and bulge stars whilst the faint peak only has bulge stars, then one would expect the kinematics of the fainter population to be more consistent with Sgr A*. However, we can see that the model does not explain the data presented in the wider view of Fig. 2. The composite bulge in the model of Joo *et al.* (2017) becomes more significant for higher $|b|$ and more negative longitudes, so we expect the kinematic differences between the two magnitude peaks to decrease. We can see that the data exhibit exactly the opposite trend with the largest kinematic difference at $(\ell, b) = (-4, -8)$ deg.

References

Bland-Hawthorn, J. & Gerhard, O. 2016, *ARA&A*, 54, 529
Clarke, J. P., Wegg, C., Gerhard, O., *et al.* 2019, arXiv e-prints
Gaia Collaboration *et al.* 2016, *A&A*, 595, A1
Gaia Collaboration *et al.* 2018, *A&A*, 616, A1

https://doi.org/10.1017/S1743921319008664 Published online by Cambridge University Press

Gonzalez, O. A., Zoccali, M., Debattista, V. P., *et al.* 2015, *A&A*, 583, L5
Joo, S.-J., Lee, Y.-W., & Chung, C. 2017, *ApJ*, 840, 98
Kozłowski, S., Woźniak, P. R., Mao, S., *et al.* 2006, *MNRAS*, 370, 435
Lindegren, L. *et al.* 2018, *A&A*, 616, A2
López-Corredoira, M., Lee, Y.-W., Garzón, F., & Lim, D. 2019, *A&A*, 627, A3
McWilliam, A. & Zoccali, M. 2010, *ApJ*, 724, 1491
Nataf, D. M., Udalski, A., Gould, A., *et al.* 2010, *ApJ*, 721, L28
Rattenbury, N. J., Mao, S., Debattista, V. P., *et al.* 2007, *MNRAS*, 378, 1165
Sanders, J. L., Smith, L., Evans, N. W., & Lucas, P. 2019a, *MNRAS*
Sanders, J. L., Smith, L., & Evans, N. W. 2019b, *MNRAS*, 488, 4552
Smith, L. C. *et al.* 2018, *MNRAS*, 474, 1826
Tremaine, S. & Weinberg, M. D. 1984, *ApJ*, 282, L5

https://doi.org/10.1017/S1743921319008664 Published online by Cambridge University Press